J|A|C|S
ARTICLES
Published on Web 11/20/2002

Conformation of Glycomimetics in the Free and Protein-Bound State: Structural and Binding Features of the *C*-glycosyl Analogue of the Core Trisaccharide α-D-Man-(1 → 3)-[α-D-Man-(1 → 6)]-D-Man

Lise Munch Mikkelsen,[†] María José Hernáiz,[‡] M. Martín-Pastor,[§] Troels Skrydstrup,*[,†] and Jesús Jiménez-Barbero*[,||]

Contribution from the Department of Chemistry, University of Aarhus, Langelandsgade 140, 8000 Aarhus C, Denmark, Instituto de Investigaciones Químicas, C.S.I.C., Isla de la Cartuja, Sevilla, Spain, Unidade Resonancia Magnética, RIAIDT, CACTUS, Santiago de Compostela, 15706 Spain, and Centro de Investigaciones Biológicas, C.S.I.C., Juan de la Cierva 3, 28006 Madrid, Spain

Received April 1, 2002

Abstract: The conformational properties of the C-glycosyl analogue of the core trisaccharide α-D-Man-(1 → 3)-[α-D-Man-(1 → 6)]-D-Man in solution have been carefully analyzed by a combination of NMR spectroscopy and time-averaged restrained molecular dynamics. It has been found that both the α-1,3- and the α-1,6-glycosidic linkages show a major conformational averaging. Unusual Φ ca. 60° orientations for both Φ torsion angles are found. Moreover, a major conformational distinction between the natural compound and the glycomimetic affects to the behavior of the ω_{16} torsion angle around the α-1 → 6-linkage. Despite this increased flexibility, the C-glycosyl analogue is recognized by three mannose binding lectins, as shown by NMR (line broadening, TR−NOE, and STD) and surface plasmon resonance (SPR) methods. Moreover, a process of conformational selection takes place, so that these lectins probably bind the glycomimetic similarly to the way they recognize the natural analogue. Depending upon the architecture and extension of the binding site of the lectin, loss or gain of binding affinity with respect to the natural analogue is found.

Introduction

Carbohydrate-protein interactions are involved in a wide variety of biological cell−cell recognition events, such as fertilization, but also potential harmful interactions, as the ones prior to a virus infection or even tumor growth.[1] Because the blocking of the viral and microbial surface lectins by suitable sugars would provide protection for such infections, the search for carbohydrate mimics has recently been the subject for much research.[2] C-Glycosyl compounds have been developed as one group of these carbohydrate analogues[3] to improve the chemical and biological stability toward hydrolytic and enzymatic degradation, by replacing the interglycosidic oxygen in the natural O-glycosides with a methylene group. In addition to the synthetic analogues, C-glycosyl compounds also appear in nature.[4] Because the substitution of an oxygen by a methylene group evidently results in a change in both the size and the electronic properties of the glycosidic and the aglyconic linkages, the flexibility and the energy barriers to rotation around the interresidual linkages are expected to change to some extent.[5] The first studies on this topic were performed by the group of Prof. Kishi[6] based on NMR analysis (mainly proton−proton vicinal coupling constants). More recently, the observation that peanut agglutinin binds basically the same conformation of C-and O-lactose induced to this research group to conclude that, in general, C- and O-glycosides share similar conformations.[7] In contrast, we and other groups have reported[8] that the synthetic C-analogues possess an increased flexibility and access a higher number of conformations in solution as compared to the natural substrates. These conformers also include those that are not in agreement with the usual orientations around Φ (Φ −60° for

* To whom correspondence should be addressed. E-mail: iqoj101@iqog.csic.es.
[†] Department of Chemistry, University of Aarhus.
[‡] Instituto de Investigaciones Químicas, C.S.I.C.
[§] Unidade Resonancia Magnética, RIAIDT, CACTUS.
[||] Centro de Investigaciones Biológicas, C.S.I.C.

(1) (a) Sears, P.; Wong, C.-H. *Angew. Chem., Int. Ed.* **1999**, *38*, 2300−2324, and references therein. (b) Gabius, H. J.; Gabius, S. *Glycosiences: Status and perspectives*; Chapman & Hall: London, 1997. (c) Varki, A. *Glycobiology* **1993**, *3*, 97−130.
(2) (a) Wirczak, Z. J. *Curr. Med. Chem.* **1999**, *6*, 165. (b) Driguez, H. *Top. Curr. Chem.* **1997**, *187*, 85. (c)Yuasa, H.; Hashimoto, H. In *Reviews on Heteroatom Chemistry*; Oae, S., Ed.; MYU: Tokyo, 1999; Vol. 19, p 35.
(3) (a) Levy, W.; Chang, D. *Chemistry of C-Glycosides*; Elsevier: Cambridge, 1995. (b) Weatherman, R. V.; Kiessling, L. L. *J. Org. Chem.* **1996**, *61*, 534. (c) Weatherman, R. V.; Mortell, K. H.; Chervenak, M.; Kiessling, L. L.; Toone, E. J. *Biochemistry* **1996**, *35*, 3619.
(4) (a) Haynes, L. J. *Adv. Carbohydr. Chem. Biochem.* **1965**, *20*, 357−369. (b) Hanessian, S.; Pernet, A. G. *Adv. Carbohydr. Chem. Biochem.* **1976**, *33*, 111−188. (c) Jaramillo, C.; Knapp, S. *Synthesis* **1994**, 1.
(5) Martin-Pastor, M.; Espinosa, J. F.; Asensio, J. L.; Jiménez-Barbero, J. *Carbohydr. Res.* **1997**, *298*, 15−49.
(6) Kishi, Y. *Pure Appl. Chem.* **1993**, *65*, 771−778.
(7) Ravishankar, R.; Surolia, A.; Vijayan, M.; Lim, S.; Kishi, Y. *J. Am. Chem. Soc.* **1998**, *120*, 11 297−11 303.
(8) Jiménez-Barbero, J.; Espinosa, J. F.; Asensio, J. L.; Cañada, F. J.; Poveda, A. *Adv. Carbohydr. Chem. Biochem.* **2001**, *56*, 235−284.

10.1021/ja020468x CCC: $22.00

α- and Φ 60° for β-linked compounds) between the glycon and the aglycon.[9] These features imply an entropy penalty in the interaction process with the corresponding protein receptor or enzyme.[10] Moreover, the protein-bound conformation of C-glycosyl compounds may differ from that recognized for the natural O-glycoside.[11] In contrast with a number of reports already published for regular C-glycosyl compounds and C-disaccharides, very limited number data are available for higher C-oligosaccharides, which in principle may show a more relevant biological relevance.[12−16] In fact, only C-trisaccharides related to blood group determinants have been analyzed.[12−14] The authors concluded that they possess a unique solution conformation, and that the conformational preferences about the two interglycosidic linkages appear to be mutually independent. Moreover, the binding affinities of these analogues toward the lectin I of Ulex Europaeus were found to be similar to those of the corresponding O-glycosides,[14] so that the authors claimed that this behavior is a proof of the conformational similarity of the corresponding O- and C-glycosyl derivatives. On the other hand, an analogue of the core trimanoside, showing only a single C-glycosyl linkage at the 1 → 6 arm, showed a highly decreased affinity[15] compared to the natural analogue**.** Surprisingly, the affinity was recovered upon substitution of the ring oxygen at the nonreducing 1 → 6 end by a sulfur atom.[15] No conformational study was performed for these compounds, and the authors explicitly stated that the NMR analysis appeared impossible due to the high overlapping of the signals.[15]

After these few and partially available data, we felt that more studies were necessary to additionally validate the use of C-glycosyl analogues as sugar mimetics and to test the conformational similarities between C- and O-glycosyl higher oligosaccharides. In this context, we decided to study a biologically relevant trisaccharide (Scheme 1), such as the C-glycosyl analogue (**1b**) of methyl 3,6-di-O−(α-D-Mannopyranosyl)-α-D-Mannopyranoside (**1a**). This model trisaccharide was chosen because of several reasons: The solution conformation of the naturally occurring core oligomannose has been studied in detail,[17] principally because this molecule not only forms one of the most commonly observed branch points in N-linked oligosaccharides, but in some cases it also forms the terminus which is directly recognized by protein receptors.[18−21] Many

Scheme 1

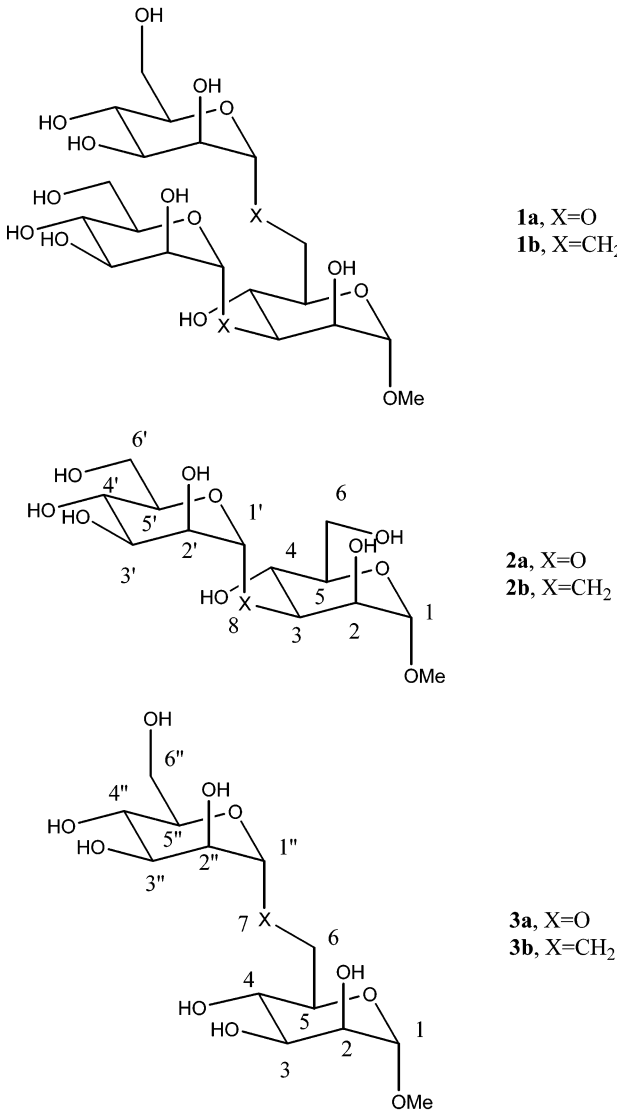

mannose binding proteins[18−21] are well-known, as concanavalin A, lentil lectin, daffodil lectin, and mannose binding protein, MBP-A. To understand how the C-glycosyl analogue can mimic the natural compound both in free solution and in the protein-bound state, we need to understand the range of 3D structures that it may adopt in water solution, as well as the relative populations of the individual conformers.

Several authors have demonstrated that the free natural O-trisaccharide[17,22,23] shows conformational averaging in solution, adopting four major and two minor geometries. Thus, the choice of this parent compound, already flexible, poses an additional point on the existence and detection of conformational differences with its C-glycosyl analogue, as well as on the relative energetics of the interaction process. Obviously, the recognition of a flexible ligand by a protein receptor will produce a restriction of motion upon binding. This fact may

(9) Asensio, J. L.; Cañada, F. J.; Kahn, N.; Mootoo, D. A.; Jiménez-Barbero, J. *Chem. Eur. J.* **2000**, *6*, 1035−1041.
(10) Searle, M. S.; Williams, D. H. *J. Am. Chem. Soc.* **1992**, *114*, 10 690−10 697.
(11) Espinosa, J. F.; Cañada, F. J.; Asensio, J. L.; Martín-Pastor, M.; Dietrich, H.; Martin-Lomas, M.; Schmidt, R. R.; Jiménez-Barbero, J. *J. Am. Chem. Soc.* **1996**, *118*, 10 862−10 871.
(12) Haneda, T.; Goekjian, P. G.; Kim, S. H.; Kishi, Y. *J. Org. Chem.* **1992**, *57*, 490−498.
(13) Wei, A.; Haudrechy, A.; Audin, C.; Jun, H.-S.; Haudrechy-Bretel, N.; Kishi, Y. *J. Org. Chem.* **1995**, *60*, 2160−2169.
(14) Wei, A.; Boy, K. M.; Kishi, Y. *J. Am. Chem. Soc*. **1995**, *117*, 9432−9437.
(15) Tsuruta, O.; Yuasa, H.; Kurono, S.; Hashimoto, H. *Bioorg. Med. Chem. Lett*. **1999**, *9*, 807−810.
(16) Berthault, P.; Birlirakis, N.; Rubinstenn, G.; Sinay, P.; Desvaux, H. J. *J. Biomol NMR*. **1996**, *8*, 23−31.
(17) (a) Brisson, J. R.; Carver, J. P. *Biochemistry* **1983**, *22*, 1362. (b) Brisson, J. R.; Carver, J. P. *Biochemistry* **1983**, *22*, 3671. (c) Brisson, J. R.; Carver, J. P. *Biochemistry* **1983**, *22*, 3680. (d) Homans, S. W.; Pastore, A.; Dwek, R. A.; Rademacher, T. W. *Biochemistry* **1987**, *26*, 6649.
(18) Sauerborn, M. K.; Wright, L. M.; Reynolds, C. D.; Grossmann, J. G.; Rizkallah, P. J. *J. Mol. Biol*. **1999**, *290*, 185−199.
(19) (a) Naismith, J. H.; Field, R. A. *J. Biol. Chem*. **1996**, *271*, 972. (b) Loris, R.; Maes, D.; Poortmans, F.; Wyns, L.; Bouckaert, J. *J. Biol. Chem*. **1996**, *271*, 30 614. (c) Bryce, R. A.; Hillier, I. H.; Naismith, J. H. *Biophys. J*. **2001**, *81*, 1373. (d) Bouckaert, J.; Hamelryck, T. W.; Wyns, L.; Loris R. *J. Biol. Chem*. **1999**, *274*, 29 188.
(20) (a) Weis, W. I.; Drickamer, K. *Annu. Rev. Biochem.* **1996**, *65*, 441−473. (b) Weis, W. I.; Kahn, R.; Fourme, R.; Drickamer, K.; Hendrickson, W. A. *Science* **1991**, *254*, 1608. (c) Weis, W. I.; Drickamer, K.; Hendrickson, W. A. *Nature* **1992**, *360*, 127.
(21) Bolon, P. J.; Al-Hashimi, H. M.; Prestegard, J. H. *J. Mol. Biol.* **1999**, *293*, 107.
(22) Almond, A.; Duus, J. O. *J. Biomol. NMR* **2001**, *20*, 351−63.
(23) Sayers, E. W.; Prestegard, J. H. *Biophys. J.* **2000**, *79*, 3313−3329.

have a negative contribution to the entropy values[24] because, in general, a less favorable entropic balance should be expected for more flexible ligands. Recent examples have provided experimental evidence on the importance of conformational preorganization of the carbohydrate ligand to improve recognition[25] by selectins or transferases.

As reviewed by Prestegard,[26] the significant NMR technological advances in recent years, as well as the presence of improved molecular dynamics (MD) force fields for carbohydrates, should be useful to perform a rigorous conformational analysis on these key glycomimetics. In this case, we have chosen to use an approach based on the characterization and measurement of the exclusive[27] interresidue NOEs[28] and *J* coupling data that define the different putative energy minima of the C-trisaccharide. These have been deduced from molecular mechanics and dynamics simulations with the AMBER*, MM3*, and AMBER 5.0 force fields.[29] The experimental data have been interpreted structurally in terms of the best-fit experimental conformer distribution, by using time-averaged restrained (tar)-MD simulations[30] using the AMBER 5.0 force field[31] and the experimental NOE/*J* information. This methodology has been rarely used in conformational analysis of oligosaccharides,[32] probably due to the lack of enough experimental constraints for these natural compounds. Usually, only one or two interresidues NOEs per glycosidic linkage are detected, which are not enough for an unambiguous definition of actual the conformational distribution. However, in the case of C-glycosyl compounds, the presence of the methylene protons at the bridge carbon permit to access to key conformational information through additional *J* and NOE data.

Therefore, herein we present the conformational study of the C-glycosyl analogue[33,34] (**1b**) of **1a** and of the *C*-glycosyl analogues of the two constituent disaccharides: methyl α-D-Man(1 → 3)α-D-Man (**2b**) and methyl α-D-Man(1 → 6)α-D-Man (**3b**). We also present the study of the interaction of **1b** with several mannose binding proteins by using both NMR (TR−NOE, STD) and SPR experiments.

Table 1. Energy, Relative Population, and Geometric Features of the Possible Conformers of **1b**, Based on the MM3*-Calculated Conformers of **2b** and **3b**[a]

conformer (population)	Φ_{13}	Ψ_{13}	$J_{1',8R}$/ $J_{1',8S}$	$J_{3,8R}$/ $J_{3,8S}$
A_{13} (36%)	−50° (exo)	55°	1.0/10.8	3.0/12.3
B_{13} (34%)	−60° (exo)	−50	2.1/11.7	11.2/1.0
C_{13} (30%)	60°(non exo)	55°	11.6/2.0	3.0/12.3
J-average			4.3/8.3	5.7/8.3
exp. *J*-(**2b**)			4.9/8.8	4.6/8.5
exp. *J*-(**1b**)			4.6/9.2	4.4/9.2

conformer (population)	Φ_{16}	Ψ_{16}	$\omega_{16(GG,20\%)}$ $J_{5,6R}/J_{5,6S}$	$\omega_{16(GT,80\%)}$ $J_{5,6R}/J_{5,6S}$	$J_{1'',7S}$/ $J_{1'',7R}$	$J_{6R,7S}$/ $J_{6R,7R}$	$J_{6S,7S}$/ $J_{6S,7R}$
D_{16} (95%)	−50° (exo)	180°	4.7/1.9	1.7/11.5	11.6/2.0	13.8/1.9	2.6/13.8
E_{16} (1%)	60°(non exo)	180°	4.7/1.9	1.7/11.5	2.7/11.6	13.8/1.9	2.6/13.8
F_{16} (4%)	−60° (exo)	60°	4.7/1.9	1.7/11.5	11.7/2.2	2.4/13.8	5.2/2.2
J-average			2.3/9.6	2.3/9.6	11.0/2.2	13.2/2.1	2.7/13.2
exp. *J*-(**3b**)			2.6/9.3	2.6/9.3	9.0/4.3	large/ small	small/ large
exp. *J*-(**1b**)			2.4/9.4	2.4/9.4	10.8/3.6	12.7/3.4	4.0/11.8

[a] Two energy and population numbers are given for the 1 → 6 linkage, one for the *gg* (expected couplings are 4.7, 1.9 Hz) and one for the *gt* (expected couplings are 1.7, 11.5 Hz) rotamers around ω_{16} of **3b**, because the Φ, Ψ values are very similar, independently of the rotamer at ω_{16}

Table 2. Energy, Relative Population, and Geometric Features of the Low Energy MM3* Conformers of **1b**[a]

conformer	Φ_{13}	Ψ_{13}	Φ_{16}	Ψ_{16}	ΔE (kJ/mol) (ω_{16})	pop(%) (ω_{16})
BD	ca. *−60*	ca. −40	ca. *−60*	anti	11.4(*gt*) 17.0(*gg*)	0.6(*gt*) 0.1(*gg*)
BF	ca. *−60*	ca. −40	ca. *−60*	ca. 60	15.2(*gt*) 23.0(*gg*)	0.1(*gt*) 0.0(*gg*)
BE	ca. *−60*	ca. −40	ca. 60	anti	14.6(*gt*) 19.5(*gg*)	0.2(*gt*) 0.0(*gg*)
AD	ca. *−60*	ca. 60	ca. *−60*	anti	0.0(*gt*) 5.6(*gg*)	**57.7**(*gt*) **6.2**(*gg*)
AF	ca. *−60*	ca. 60	ca. *−60*	ca. 60	3.7(*gt*) 11.6(*gg*)	**13.2**(*gt*) 0.6(*gg*)
AE	ca. *−60*	ca. 60	ca. 60	anti	3.1(*gt*) 8.3(*gg*)	**16.8**(*gt*) **2.1**(*gg*)
CD	ca. 60	ca. 60	ca. *−60*	anti	9.2(*gt*) 14.9(*gg*)	**1.5**(*gt*) 0.2(*gg*)
CF	ca. 60	ca. 60	ca. *−60*	ca. 60	13.1(*gt*) 20.9(*gg*)	0.3(*gt*) 0.0(*gg*)
CE	ca. 60	ca. 60	ca. 60	anti	12.4(*gt*) 17.6(*gg*)	0.4(*gt*) 0.0(*gg*)

[a] They are formed by combination of the three (A, B, C) found conformers for **2b** and the three (D, E, F) for **3b**. Two energy and population numbers are given, one for the *gg* and one for the *gt* rotamers around ω_{16} because the Φ, Ψ values are very similar independently of the rotamer at ω_{16}. Major conformers are emboldened.

Conformational Features of the C-Trisaccharide and Its Constituent C-Disaccharides

Molecular Mechanics and Dynamics Analysis with the MM3* Force Field. The potential energy Φ/Ψ surfaces for **2b** and **3b** were calculated with MM3* as integrated in MACROMODEL,[35] and compared to those of their parent O-glycosides (**2a** and **3a**), as discussed in the Supporting Information (see also Table 1). Three minima are predicted for **2b** and six more for **3b**. Then, the conformational behavior of **1b** was analyzed. In a first step, molecular mechanics and dynamics calculations with the MM3* program and the GB/SA water solvent model were performed, for the eighteen basic possible conformations of the C-trisaccharide [three (**2b**) multiplied by six (**3b**)], as discussed in the Supporting Information (see also Table 2). As conclusion, a combination of 6 conformational families was predicted to coexist from these MM3*-MD simulations with more than 1% of population. Therefore, two additional families, apart of those described for **1a** do appear in the simulation. Geometrical parameters (especially, torsion angles, single and ensemble average dis-

(24) (a) Yu, Y. B.; Privalov, P. L.; Hodges, P. S. *Biophys. J.* **2001**, *81*, 1632. (b) Karplus, M.; Janin, J. *Protein Eng.* **1999**, *12*, 185.
(25) (a) Thoma, G.; Magnani, J. L.; Patton, J. T.; Ernst, B.; Jahnke, W. *Angew. Chem., Int. Ed.* **2001**, *40*, 1941−1945. (b) Galan, M. C.; Venot, A. P.; Glushka, J.; Imberty, A.; Boons, G.-J. *J. Am. Chem. Soc*. **2002**, *124*, 5964−5973.
(26) Prestegard, J. H. *Nature Struct. Biol*. **1998**, *6*, 517−523.
(27) Dabrowski, J.; Kozar, T.; Grosskurth, H.; Nifant′ev, N. E. *J. Am. Chem. Soc*. **1995**, *117*, 5534.
(28) Neuhaus, D.; Williamson, M. P. *The NOE Effect in Structural and Conformational Analysis*; VCH: New York, 1989.
(29) For a discussion on the application of molecular mechanics force fields to sugar molecules, see Perez, S.; Imberty, A.; Engelsen, S.; Gruza, J.; Mazeau, K.; Jimenez-Barbero, J.; Poveda, A.; Espinosa, J. F.; et al. *Carbohydr. Res.* **1998**, *314*, 141−155.
(30) (a) Torda, A. E.; Scheek, R. M.; van Gunsteren, W. F. *J. Mol. Biol*. **1990**, *214*, 223−235. (b) Pearlman, D. A. *J. Biomol. NMR* **1994**, *4*, 1−16.
(31) (a) Pearlman, D. A.; Case, D. A.; Caldwell, J. W.; Ross, W. S.; Cheatham, T. E.; DeBolt, S.; Ferguson, D.; Siebal, G.; Kollmann, P. A. *Comput. Phys. Commun.* **1995**, *91*, 1−41. (b) Pearlman, D. A.; Kollmann, P. A. *J. Mol. Biol.* **1991**, *220*, 457−479.
(32) Asensio, J. L.; Garcia, A.; Murillo, M. T.; Fernández-Mayoralas, A.; Cañada, F. J.; Johnson, C. R.; Jiménez-Barbero, J. *J. Am. Chem. Soc*. **1999**, *121*, 11 318−11 329.
(33) (a) Mikkelsen, L. M.; Krintel, S. L.; Jimenéz-Barbero, J.; Skrydstrup, T. *Chem. Commun.* **2000**, 2319. (b) Krintel, S. L.; Jimenéz-Barbero, J.; Skrydstrup, *Tetrahedron Lett.* **1999**, *40*, 7565. (c) Krintel, S. L.; Jimenéz-Barbero, J.; Skrydstrup, *J. Org. Chem.* **2002**, *67*, 6297−6308.
(34) For a perspective on the problematic of deducing oligosaccharide conformations by NOE measurements, see for instance, (a) Peters, T.; Pinto, B. M. *Curr. Opin. Struct. Biol.* **1996**, *6*, 655. (b) Poveda, A.; Asensio, J. L.; Martín-Pastor, M.; Jimenez-Barbero, J. *J. Biomol. NMR* **1997**, *10*, 29−43.
(35) Mohamadi, F.; Richards, N. G. J.; Guida, W. C.; Liskamp, R.; Caufield, C.; Chang, G.; Hendrickson, T.; Still, W. C. *J. Comput. Chem.* **1990**, *11*, 440−467.

Table 3. Calculated Coupling Constants (Haasnoot-Altona) in Comparison with the Experimental Ones for **1b**, **2b**, and **3b** (in Hz)[a]

	$J_{H1''-H7R}$	$J_{H1''-H7S}$	J_{H5-H6R}	J_{H5-H6S}	$J_{H1'-H8R}$	$J_{H1'-H8S}$	J_{H3-H8R}	J_{H3-H8S}
2b					4.9	8.8	4.6	8.5
3b	4.3	9.0	2.6	9.3				
1b (MD -MM3*)	4.91	8.58	2.46	10.06	5.40	8.04	6.28	7.18
1b (AMBER water box)	3.72	9.90	2.05	10.97	3.44	8.56	4.97	8.47
1b (tar-AMBER *J*s and NOEs)	3.21	10.25	2.70	9.22	3.98	9.10	4.46	8.77
1b (exp. 800 MHz)	3.6	10.8	2.6	9.4	4.6	9.2	4.4	9.2

[a] The values for the MD-MM3* analysis, for the solvated simulation and for the tar-MD approach are given in different rows.

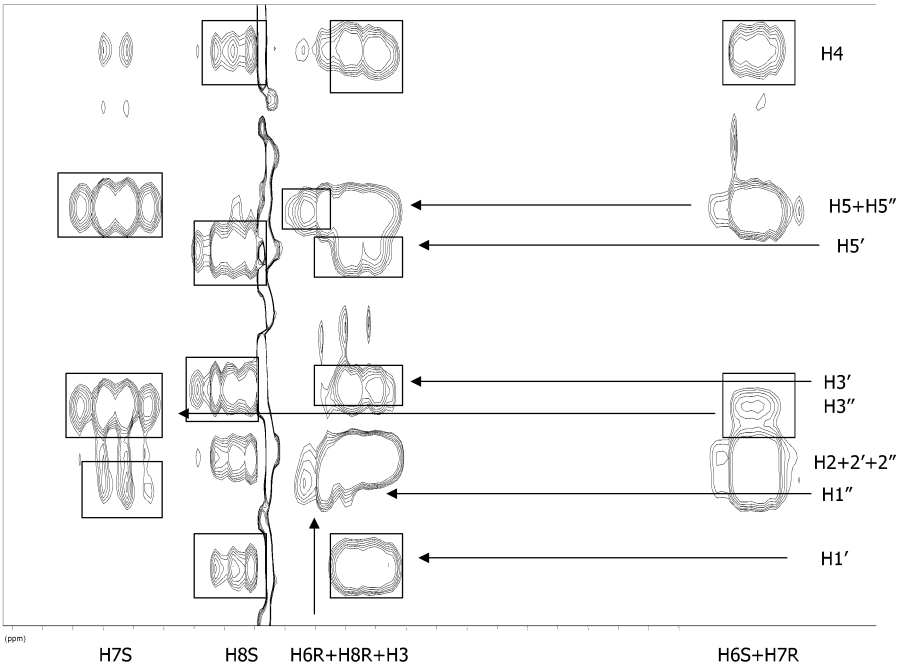

Figure 1. Expansion of the sugar proton/methylene region of the T-ROESY spectrum (mixing time 400 ms) carried out at 700 MHz for C-trisaccharide **1b**. Key NOE cross-peaks are highlighted. Cross-peak volumes were estimated using the software provided by the manufacturer.

tances, $\langle r^{-6}\rangle^{-1/6}$) were extracted from the obtained geometries and trajectories to be compared with the those corresponding to the experimental NMR parameters. Thus, the sampled MM3*-based MD trajectories were used to derive the expected $^3J_{HH}$ by applying the Haasnoot−Altona modification of the Karplus equation.[36,37]

NMR Data. Then, the NMR data were acquired and analyzed to verify if the MM3* calculations were able to quantitatively reproduce the experimental data. The key NMR data in D_2O of compound **1b** and of its two constituent disaccharides (**2b** and **3b**) are listed in Table 3 and in the Supporting Information. NMR data (*J* and NOEs) for **2b** and **3b** were obtained at 500 MHz. For the C-trisaccharide (**1b**), the use of high field NMR (700 and 800 MHz) was necessary to partially solve the proton overlap for the methylene and aglyconic protons surrounding the pseudo-glycosidic linkages (Figure in the Supporting Information). In this way, the 1D spectrum was amenable to computer simulation and the best *J* values for **1b** could be extracted and compared to those expected for the geometries deduced from the calculations. The NOEs for **1b** were derived from a series of 700 MHz T-ROESY spectra (see Figure 1 and Supporting Information). The experimental NOEs were translated into distances and compared to those extracted from the MM3* calculations, for single conformers and for ensemble average distributions. The important NOEs are also summarized in Table 4, together with the conformation/s that they represent. The unambiguous assignment of the prochiral methylene protons attached at both bridges[38] and at C-6 of ω_{16} torsion angle was exclusively based on the experimental *J* and NOE data, following the protocol described in the Supporting Information.

Discussion

Comparison of the NMR Data to those Extracted from MM3*. The *J* values for the ring protons indicate that all the pyranose rings adopt the usual $^4C_1$ chair, independently of the size of the molecule and of the nature of the C-glycosidic linkage. Although, this is usually the case, in some cases alternative chair conformations have been described for other C-glycosyl compounds.[39] The coupling constants also afford information on the conformational distribution around the torsional[36,37] degrees of freedom of the molecule (Φ, Ψ, and ω angles). From the inspection of the *J* values, (Table 3 and Figures in the Supporting Information) it can be deduced that those for **1b** are relatively similar to those of the separate C-disaccharides, **2b** and **3b**. Importantly, there is a significant change in the coupling values around ω_{16} (J_{H5-H6R}, J_{H5-H6S}),

(36) Karplus, M. *J. Chem. Phys*. **1959**, *30*, 11−20.
(37) Haasnoot, C. A. G.; De Leeuw, F. A. A. M.; Altona, C. *Tetrahedron* **1980**, *36*, 2783−2794.
(38) (a) Nishida, Y.; Ohrui, H.; Meguro, H. *Tetrahedron Lett.* **1984**, *25*, 1575. (b) Ohrui, H.; Nishida, Y.; Itoh, H.; Meguro, H. *J. Org. Chem*. **1991**, *56*, 1726. (c) Bock, K.; Duus, J. *J. Carbohydr. Chem*. **1994**, *13*, 513−543.
(39) Carpintero, M.; Bastida, A.; Garcia-Junceda, E.; Jimenez-Barbero, J.; Fernandez-Mayoralas, A. *Eur. J. Org. Chem*. **2001**, 4127−4135.

Table 4. Experimental NOEs and Corresponding Interproton Distances of **1b** as Estimated from T-ROESY Experiments (mixing times of 300, 400, and 500 ms) and a full matrix relaxation approach, at 700 MHz in D_2O and 303 K

proton pair	intensity	experimental distance	Φ ca −60° (*gg* or *gt*)	Φ ca. 60°	TRNOE lentil/**1b**	TRNOE daffodil/**1b**
					intensity	intensity
H5′−H8S	ms	2.6−2.8	2.1	2.9*	vw (C)	w (C)
H2,2′,2″−H8S	mw	2.8−3.0	3.3	3.1	vw	
H1′−H8S	mw	2.8−3.0	3.1	2.5*	vw (A,B)	− (A,B)
H3′−H8S	ms	2.6−2.8	2.5	3.9	ms (A,B)	ms (A,B)
H4−H8S	weak	3.0−3.2	3.1	3.1	vw	
H3′−H8R	m	2.7−2.9	3.1	2.3*	m	m
H4−H8R,3	ms	2.6−2.8	2.6	2.6	m	m
H1′-H8R, 3	s	2.3−2.6	2.4	3.1	m (A,B)	mw
H2′,2,2″-H8R,3	ms	2.6−2.8	2.3	2.3	s	s
H5′−H8R	mw	2.8−3.0	3.6	2.9	w	w
H5−H8a, 3	ms	2.6−2.8	2.5	2.5	s	s
H2″−H6R	w	3.0−3.2	4.7−4.4	2.2−3.3*	s**(H2/H3)	s**(H2/H3)
H5,5″−H6R	ms	2.6−2.8	2.5	2.5	s**(H3/H5)	s**(H3/H5)
H4−H6R	w	3.0−3.2	3.8−3.1	3.8−3.1	m*	m*
H1″−H6R	m	2.7−2.9	2.5	3.0*	ms (D,F)	m (D,F)
H3″−H7R,6S	mw	2.8−3.0	3.2/4.5	2.2*	w (D,F)	vw (D,F)
H2″−H7R,6S	ms	2.6−2.8	2.5	3.2	ms (D,F)	ms (D,F)
H1″−H7R,6S	s	2.3−2.6	2.5/3.1	3.1/2.5	s	s
H5,5″−H7R,6S	s	2.3−2.6	2.5	2.1	ms	mw
H4−H7R,6S	ms	2.6−2.8	2.5	2.5	m	mw
H3″−H7S	s	2.3−2.6	2.2	3.8	s (D,F)	s (D,F)
H4−H7S	vw	3.1−3.4	2.2−4.4	2.2−4.4	− (gt)	− (gt)
H5,5″−H7S	s	2.3−2.6	2.1	2.8	w	vw
H1″−H7S	mw	2.8−3.0	3.1	2.5	vw (D,F)	w (D,F)
H1″−H5	vw	3.1−3.4	2.2 (if Ψ 60°)	>4	- (E)	- (E)

The experimental distanves were included in the tar-MD dynamics, additionally expanding the allowed range in 0.1 Å both ways. The expected distances for the different conformers a−i are also given to evaluate the presence of a given geometry. In the final two columns, the TR−NOE intensities for **1b** complexed to lentil and daffodil lectins are also given, together with the conformations that they represent (see text). The ** indicate overlapping. Many peaks can only be explained by conformers of the type A, B (1,3-linkage) and D, E, F (1,6-linkage), with Φ angles ca. −60°, and *gt* orientations for the ω_{16} torsion, respectively.

when those measured for **1b** and **3b** are compared to those described for the natural analogues. The values increase from ca. 2.2 and 5.5 Hz in **1a**[17] to ca. 2.5 and 9.0 Hz, for J_{H5-H6R} and J_{H5-H6S}, respectively, in **1b** and **3b**. These changes indicate that the ω_{16} torsions in the C-glycosides adopt better-defined orientations[37] with respect to those in the natural compound, **1a**. The other *J* values (Tables 1 and 3 and Supporting Information) are also in agreement with a rigidification of the glycosidic linkages of **1b** with respect to both disaccharides, thus providing a first indication of a certain degree of correlation between both glycosidic linkages. The key point here is that just with the use of *J* information, it is possible to deduce some restriction to the motion around the glycosidic linkages in **1b** with respect to those in the isolated C-disaccharides. Only NOE information is available for O-glycosides in isotropic medium, and the subtle changes deduced from the *J*-analysis of **1b** could have no translation into differences of NOE values, due to the intrinsic experimental error and to the variations in global and internal motion correlation times, when passing from di to trisaccharides.[34]

Regarding NOEs (Table 4), it was possible to observe NOEs characteristic for all the different calculated minima in terms of Φ/Ψ, evidencing that they all coexist in solution. Deconvolution of the data to afford their relative populations was not possible at this stage.

Thus, this starting analysis of the NMR data permitted to identify a major *gt* rotamer around ω_{16} of the C-trisaccharide (and in the constituent **3b** disaccharide), the presence of major regular Φ ca. −60° rotamers around all Φ linkages in the three compounds, the presence of equilibria around Ψ_{13} linkages, and a major anti orientation around Ψ_{16}. Nevertheless, a more quantitative characterization of all the possible conformers in the conformational equilibrium and of their relative populations is necessary to properly understand its binding properties. When the comparison between expected and experimental vicinal proton−proton couplings was performed, some of the calculated couplings deviate more than 1 Hz from the experimental results, marked in bold in the Table 3. Indeed, the MM3*-based MD predict a higher percentage of unusual Φ ca. 60° conformers around both glycosidic linkages, than those actually existing. Moreover, they also predict a higher flexibility around Ψ_{13}, (averaging of both $J_{3,8}$ couplings) than that experimentally observed (one large and one medium-small *J*).

Comparison of the NMR Data to those Extracted from Solvated MD Simulations with the AMBER 5.0 Force Field. Therefore, to try to improve the fitting between experimental and expected data, we decided to perform additional MD simulations (s-MD), now using explicit water molecules and the AMBER 5.0 force field with the GLYCAM parameters for the carbohydrate portion of **1b**.[40,41] As starting structure, the different glycosidic linkages were set at the A_{13}, D_{16}, and *gt* (ω_{16}) conformers (See Table 1). The s-MD plots are given in Figure 2. Also in this case, a conformational equilibrium of 6 major basic geometries is predicted in water, although with different populations to those given by MM3*. The corresponding expected and observed *J* values are shown in Table 3. There is a fair matching between both sets of data, better than that observed with the MM3*-based simulations, but the agreement is not perfect, with deviations higher than 1 Hz in two cases,

(40) Woods, R. J.; Edge, C. J.; Dwek, R. A. *Nature Struct. Biol.* **1994**, *1*, 499.
(41) Kirschner, K. N.; Woods, R. J. *Proc. Natl. Acad. Sci. U.S.A.* **2001**, *98*, 10 541.

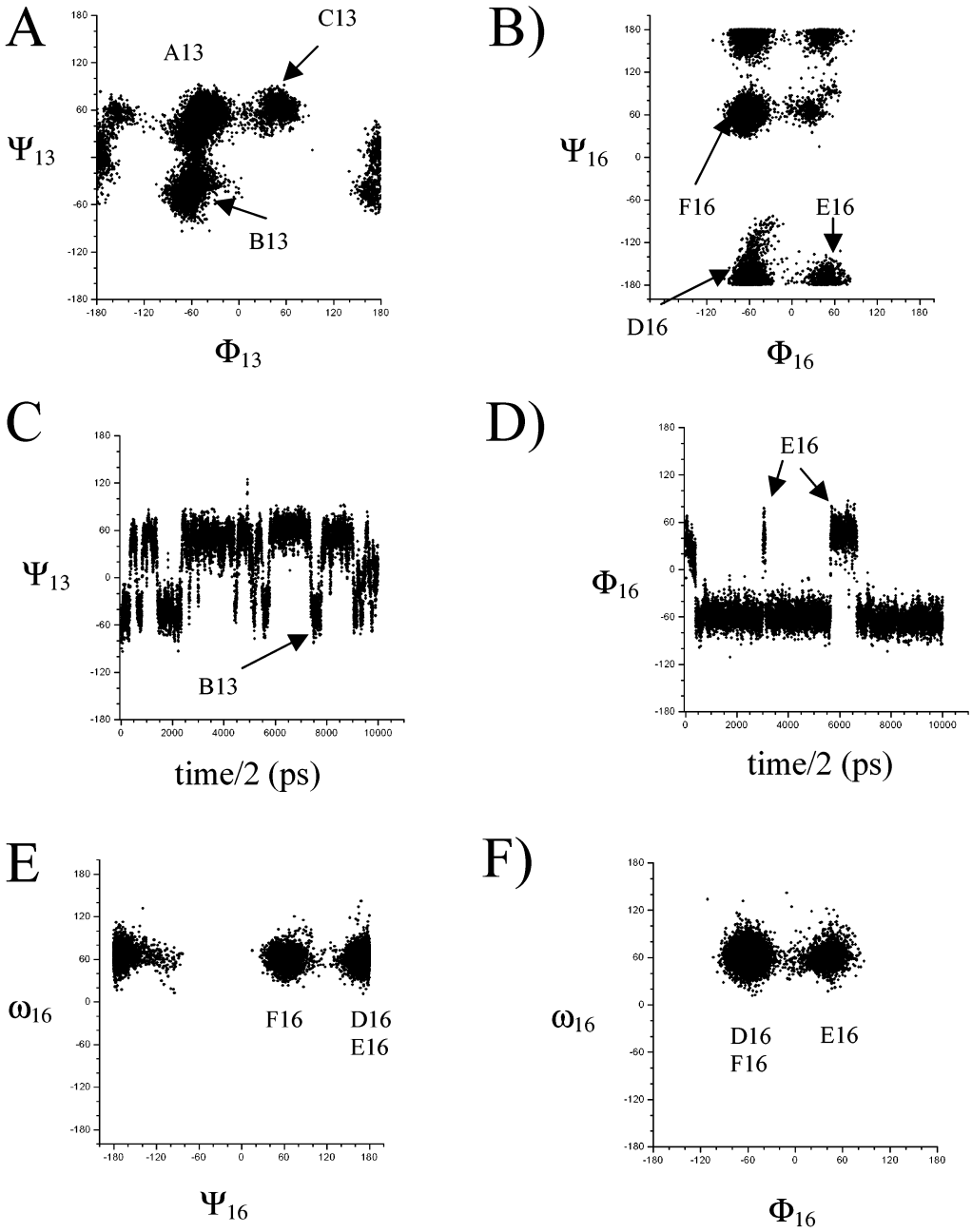

Figure 2. Trajectory Φ/Ψ plots from the solvated MD simulations carried out for the C-trisaccharide (**1b**) with the AMBER 5.0 force field (explicit water) force field. In total, this figure covers a simulation time of 5.6 ns. (A) Φ_{13} vs Ψ_{13}. (B) Φ_{16} vs Ψ_{16}. (C) Ψ_{13} vs time. (D) Φ_{16} vs time. (E) ω_{16} vs Φ_{16}. (F) ω_{16} vs ψ_{16}.

marked in bold in Table 3. It seems that the simulation time is not large enough to adequately reproduce the experimental results, which are obviously reflecting motions that take place over very large time scales.[41] As leading example, the experimental conformational equilibrium around the exocyclic C5−C6 linkages of simple monosaccharides, glucose, and galactose has been recently reproduced by a solvated 50 ns simulation with the AMBER 5.0 force field.[41] For a pseudotrisaccharide such as **1b**, the time scale of the fluctuation around ω_{16} is not necessarily the same than that for a monosaccharide, and the simulation time for convergence could be longer.

Time Averaged Restrained Molecular Dynamics (AMBER 5.0). Therefore, we decided to use an alternative method to get the best fit to the experimental NMR data. Thus, time averaged restrained (tar) MD-calculations[30] with the AMBER 5.0 force field were performed.[9,31,32]

As mentioned above, exclusive NOEs of regular Φ ca. −60° conformations around Φ_{13} and Φ_{16}, coexist with other exclusive for unusual Φ ca. 60° forms, and also NOEs exclusive for Ψ_{16} close to 60° are also evident (Table 4). NOEs favoring the gt orientation around ω_{16} are also stronger than those that are due to a *gg* disposition. These NOEs were included in the tar-MD AMBER calculations, together with the observed coupling constants. The calculation was first run on a 15 ns time scale and then on a 56 ns time scale to get a better convergence (Figures 3 and 4). The final coupling constants are listed in Table 3 to evaluate the improvement achieved when passing from the solvated simulations to the tar-MD ones. The results

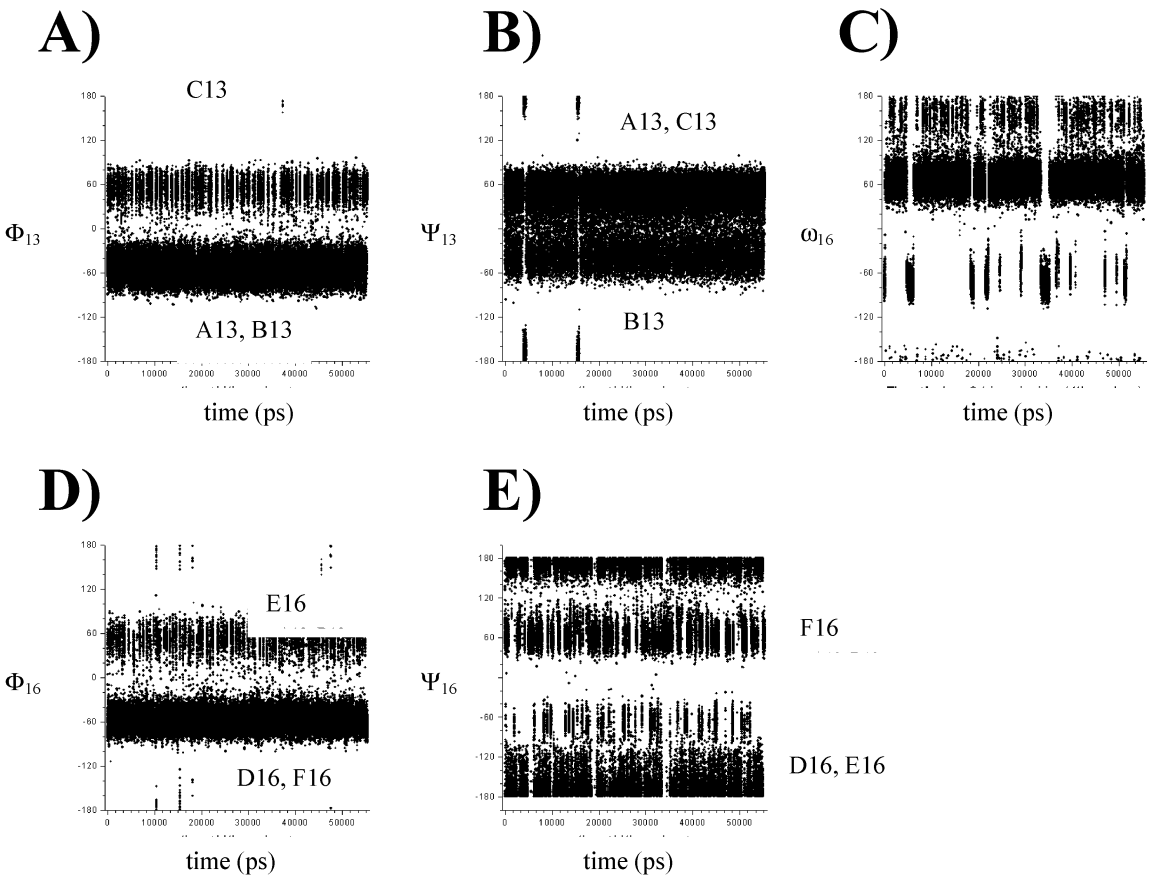

Figure 3. Details of the trajectory Φ/Ψ plots from a tar-MD simulations carried out for the C-trisaccharide (**1b**) with the AMBER 5.0 force field for 56 ns and the J and NOE restrictions discussed in the text. (A) Φ_{13} vs time. (B) Ψ_{13} vs time. (C) ω_{16} vs time. (D) Φ_{16} vs time. (E) Ψ_{16} vs time.

from this latter calculation, which showed no violations (Table S3 in Supporting Information) of the desired values of the coupling constants or of the inter-proton distances (NOEs), are also listed in Table 4. Therefore, under these conditions, the tar-MD calculations are able to reproduce the actual conformation of the C-trisaccharide in aqueous solution with very good accuracy.

It is noteworthy to point out that the small amount of Ψ_{13} close to 180° present in shorter trajectories are only temporary points because in the long (56 ns) run, the observation of this specific value disappears completely after approximately 15 ns and do not appear later on. This observation indicates the importance of sampling over a large period of time.

Therefore, the conformational behavior of **1b** in water may be described as a conformational ensemble of six basic forms, whose populations oscillate between 2 and 40%. Unusual Φ ca. 60° conformers are unequivocally present in solution in ca. 15% population, in contrast to the natural O-glycosyl analogue (less than 1%). Therefore, on a semiquantitative basis, the free energy difference due to the stereoelectronic component of the exo-anomeric effect amounts to about 1.6 kcal/mol, in good agreement with the data previously reported by us for simple C-disaccharides.[9,32] Due to this high flexibility, even higher than that reported for the natural compound,[23] it is expected that the interaction of **1b** with protein receptors may be penalized due to entropic factors, always depending on the topology of the binding site.

Similarly to the description provided by Prestegard for **1a**, the major conformations arise from several transitions, at the α(1 → 3) and the α(1 → 6) linkages. The comparison of the data for **1b** with those obtained for **2b** and **3b** suggest that the changes at either glycosidic linkage are correlated with each other.

Binding Studies

Now, having observed that the solution behavior of **1b** is different than that of its parent **1a**, it becomes interesting to verify whether the C-trisaccharide is still able to bind to different mannose-binding lectins. NMR and SPR studies were used to this aim. It has previously been described that C-glycosides are able to bind to enzymes and lectins.[8,14,42,43] Depending upon the nature and the topology of the protein binding site, either similar or rather distinct conformations of the O/C-pair of compounds are bound.[44,45] For testing **1b** as glycomimetic, three different mannose binding proteins were selected: concanavalin A (from *Canavalia ensiformis* (Jack bean)), lentil lectin (from *Lens culinaris*) and the lectin from *Narcissus pseudonarcissus* (Daffodil flower). All of them display selectivity toward O-mannopyranosyl residues.[18,19] Moreover, the X-ray structures of these lectins bound to disaccharides and trisaccharides are

(42) Asensio, J. L.; Espinosa, J. F.; Dietrich, H.; Cañada, J.; Schmidt, R. R.; Martín-Lomas, M.; André, S.; Gabius, H.-J.; Jiménez-Barbero, J. *J. Am. Chem. Soc.* **1999**, *121*, 8995−9000
(43) Weatherman, R. V.; Mortell, K. H.; Chervenak, M.; Kiessling, L. L.; Toone, E. J. *Biochemistry* **1996**, *35*, 3619−3624.
(44) Espinosa, J. F.; Montero, E.; Vian, A.; Garcia, J. L.; Dietrich, H.; Schmidt, R. R.; Martin-Lomas, M.; Imberty, A.; Cañada, J.; Jimenez-Barbero, J. *J. Am. Chem. Soc.* **1998**, *120*, 1309−1316.
(45) García-Herrero, A.; Montero, E.; Muñoz, J. L.; Espinosa, J. F.; Vián, A.; García, J. L.; Asensio, J. L.; Cañada, F. J.; Jiménez-Barbero, J. *J. Am. Chem. Soc.* **2002**, *124*, 4804−4810.

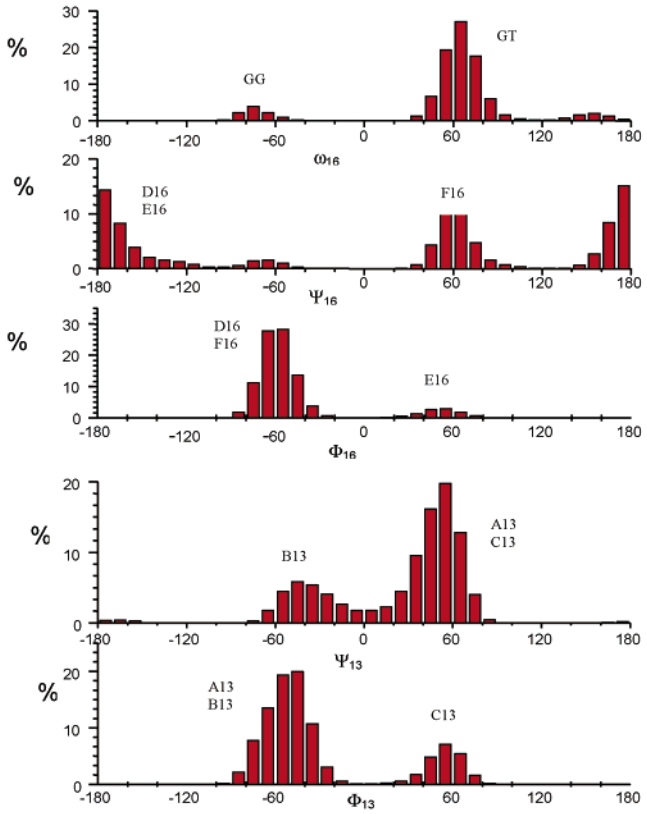

Figure 4. Population histograms from the trajectory Φ/Ψ plots from the tar-MD simulations carried out for the C-trisaccharide (**1b**) with the AMBER 5.0 field for 56 ns and the J and NOE restrictions discussed in the text. They show that there are substantial amounts of Φ +60° conformations, never found in the parent *O*-glycosides. (A) From top to bottom, ω_{16}, Ψ_{16}, Φ_{16}, Ψ_{13}, and Φ_{13}.

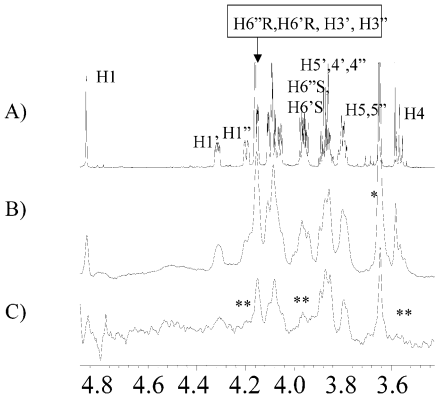

Figure 5. Details of the 1D 1H NMR STD spectra of **1b**, complexed to daffodil lectin. (A) top: the free state at 299 K. (B) Spectrum for the complex 1b/daffodil lectin (34:1). (C) STD spectrum for the complex 1b/daffodil lectin (34:1). The shown results are obtained after irradiation at the region of the protein envelope. It is observed that the protons belonging to the terminal non reducing moieties are more intense than those belonging to the reducing mannose unit. Protons that virtually disappear (the position of H-4 of this residue) are marked with **). The * point to impurities of the preparation that do not appear in the STD spectra, due to the fact that they are not bound to the lectin.

available. In particular, structures of **1a**, **2a**, and **3a** bound to Con A have been described,[19] whereas one of **2a** bound to Daffodil lectin has been deposited.[18] No structure of lentil lectin bound to either **1a**, **2a** or **3a** have been documented, although the structure of this lectin bound to sucrose is available.[46] Lentil lectin also binds Glc moieties.

To test the binding, 1D ^{1}H NMR spectra were recorded after additions of the three lectins to the NMR tubes containing **1b** dissolved in a D_2O buffer (Figures in the Supporting Information). All lectins caused a significant line broadening of the C-glycosyl signals, thus providing a clear indication of the existence of binding. As a further step, and to identify the structural and conformational features of the binding process, saturation transfer difference (STD) experiments (epitope mapping[47,48]) and NOESY (bound conformation[49]) spectra were also recorded.

Concanavalin A has a binding site specific for **1a** and, moreover, accurate binding data are available.[50] The analysis of the crystal structure published by Naismith[19a] and Loris et al.[19b] of the complex of Con A with **1a** reveals that no important hydrogen bonding is present that involves the two interglycosidic oxygens. Interactions between the three sugar moieties and the polypeptide chain are evident in the X-ray structure. Therefore, the existing differences between the O- and C-trisaccharides if any, should reflect the distinct conformational behavior between **1a** and **1b**. In particular, the four binding sites show that all **1a** molecules show a gg orientation around ω_{16}, in contrast with the major gt orientation of this angle for **1b** in solution.

STD experiments were then performed to try to identify the binding epitope.[47,48,51] For the Con A/**1b** complex, no clear differences in the response of the three Man residues were observed upon saturation with different power or increasing saturation time. Therefore, this observation seems to indicate that the three Man residues are indeed effectively bound by the lectin. In fact, this observation agrees with the X-ray structure of the complex of this lectin with **1a**, for which there are relevant contacts of the polypeptide chain with the three Man residues. Therefore, the glycomimetic seems to be bound by Con A in an analogous manner to the natural compound.

Similarly, STD spectra were recorded for the complexes of **1b** with lentil and daffodil lectins. These spectra are shown in Figure 5 and in the Supporting Information. In both cases, for saturation times up to 500 ms, the magnetization was transferred to only the protons belonging to both nonreducing ends. For instance, as shown in Figure 5, it is clear that H4 (3.32 ppm) of the reducing sugar is not observed in the difference spectrum, whereas, except both anomeric protons, the signals from the two nonreducing ends do appear. Therefore, these two lectins seem to mainly recognize the two arms of the glycomimetic. Indeed, the lack of recognition of the three residues is consistent with previous reports describing that daffodil lectin recognizes linear than branched trimannoses.[52a] Although this daffodil lectin is best bound by α-1 → 6 linked manno-oligosaccharides,[52b] it

(46) Casset, F.; Hamelryck, T.; Loris, R.; Brisson, J. R.; Tellier, C.; Dao-Thi, M. H.; Wyns, L.; Poortmans, E.; Perez, S.; Imberty, A. *J. Biol. Chem.* **1995**, *270*, 25 619.
(47) Meyer, M.; Meyer, B. *Angew. Chem., Int. Ed. Engl.* **1999**, *38*, 1784−7.
(48) Klein, J.; Meinecke, R.; Meyer, M.; Meyer, B. *J. Am. Chem. Soc*., **1999**, *121*, 5336−5337.
(49) For the use of TRNOE experiments in the study of protein carbohydrate interactions, see for instance, (a) Bevilacqua, V. L.; Thomson, D. S.; Prestegard, J. H. *Biochemistry* **1990**, *29*, 5529; (b) Poveda, A.; Jimenez-Barbero, J. *Chem. Soc. Rev.* **1998**, *27*, 133−143.
(50) Gupta, D.; Dam, T. K.; Oscarson, S.; Brewer, C. F. *J. Biol. Chem.* **1997**, *272*, 6388.
(51) Vogtherr, M.; Peters, T. *J. Am. Chem. Soc*. **2000**, *122*, 6093−6099.
(52) (a) Kaku, H.; Goldstein, I. J. *Carbohydr. Res.* **1992**, *229*, 346. (b) Kaku, H.; Goldstein, I. J.; Oscarson, S. *Carbohydr. Res*. **1991**, *220*, 109. (c) Kaku, H.; Van Damme, E. J.; Peumans, W. J.; Goldstein, I. J. *Arch. Biochem. Biophys.* **1990**, *279*, 298−304.

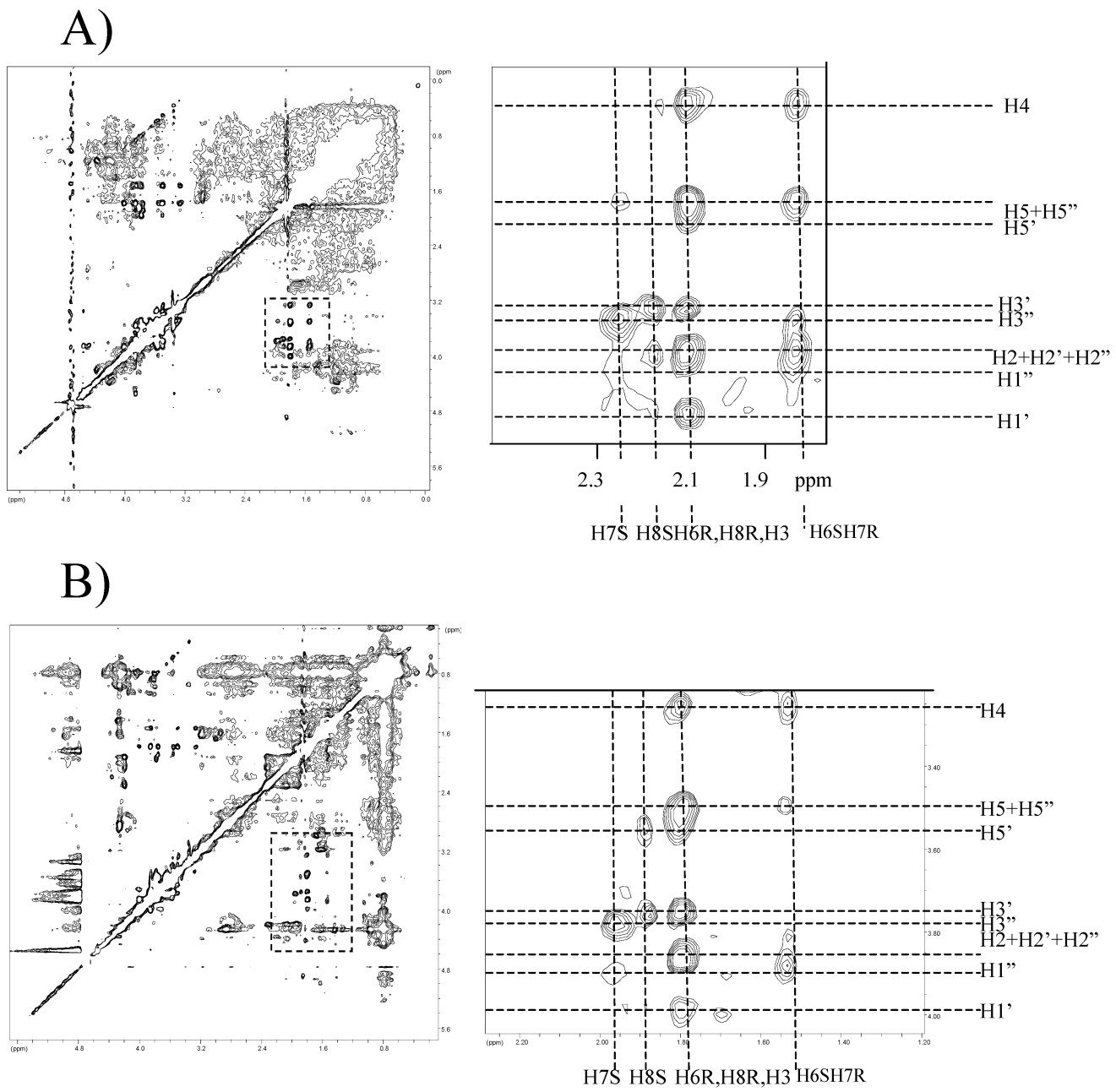

Figure 6. (a) TR−NOESY spectrum (500 MHz, 150 ms mixing time) of **1b** complexed to lentil lectin (molar ratio 17:1) at 296 K. (b) Expansion of the key region showing the relevant cross-peaks. The cross-peaks corresponding to exoanomeric conformers around both Φ angles are observed, indicating the preferred recognition of the natural exo-anomeric conformers. (b) TR−NOESY spectrum (500 MHz, 150 ms mixing time) of **1b** complexed to daffodil lectin (molar ratio 34:1) at 296 K. (b) Expansion of the key region showing the relevant cross-peaks. The results are virtually identical to those observed in for the lentil complex. The cross-peaks corresponding to exoanomeric conformers around both Φ angles are observed, indicating the preferred recognition of the natural exo-anomeric conformers.

also recognizes α-1 → 3-mannose units, as shown in the recently available crystal structure of the daffodil/**2a** complex.[18] Here, one of the binding sites does not show interactions between the polypeptide chain and the nonreducing end. Therefore, the STD-based observation of a distinction between the terminal ends and the reducing Man moieties of **1b** is not unexpected. Regarding lentil lectin, its X-ray structure bound to sucrose shows major contacts between the Glc unit and the protein, while the fructose moiety remains of the binding site. These data are in close agreement with the observations of the STD experiments.

As a further step, TR−NOESY experiments were attempted to deduce the bound conformation of **1b** in the three cases. No TR−NOE experiments have been ever described for Con A complexes, probably due to the presence of a paramagnetic manganese ion relatively close to the binding site, and neither was TR−NOE observed for the Con A/**1b** complex. Therefore, although the STD experiments suggest that the structural features of the binding of **1b** to ConA may be similar to those of **1a** in the crystal, no insights on the binding of either regular Φ ca. −60° or unusual Φ ca. 60° conformers of **1b** may be extracted.

Table 5. SPR Data for the Interaction of Con A and Daffodil Lectins with **1b**

lectin	k_{on} (M^{-1} s^{-1})	k_{off} (s^{-1})	K_d (M) (**1b**)	K_d (M) (**1a**)[51,53]
Concanavalin a.	1.85×10^3	0.24	1.3×10^{-4}	2×10^{-6}
daffodil	0.43×10^3	0.23	5.2×10^{-4}	1.5×10^{-3}

In contrast, TR−NOE cross-peaks were observed for the complexes of **1b** with both lentil and *Narcissus pseudonarcissus* lectins. The negative cross-peaks in the TR−NOESYs (Figure 6) contain the conformational information of the bound glycomimetic.[49] Both sets of TR−NOE cross-peaks, at several mixing times, were very similar, and somehow different from that observed in the free state (see the comparison with Figure 1). Indeed, several signals present in the free state do not longer appear in the spectra for the complexes. Therefore, and as a first approximation, it can be deduced that a case of conformational selection is taking place, i.e., only one or some conformations of those present in the free state are preferentially bound by these lectins. Moreover, the experimental data also indicate that these two mannose-binding proteins select the same type/s of conformation/s. The observed NOEs are also listed in Table 4 along with their representative conformers. A quantitative analysis was attempted using a full relaxation matrix approach, but indeed it was not possible to fit the cross-peak volumes for the different linkages using a single correlation time. This fact is not unexpected because mobility can still exist in the binding site, so that the different proton pairs have different effective correlation times.

The observed cross-peaks (Table 4) mainly correspond to glycosidic torsion angles (Φ_{13} and Φ_{16}) in the vicinity of −60°. That is, both lectins select preferentially regular conformers at both glycosidic angles. The binding of unusual Φ ca. 60° conformers in a extent about 5−10% cannot be discarded either because some of the cross-peaks (especially, H5p−H8S) may also be representative of a small population of these geometries. Moreover, the *gt* conformer around ω_{16} seems also to be preferentially selected because no H-4/H-7S cross-peak is observed, that is exclusive of the gg conformer. Therefore, it can be pointed out that, despite the fact that the glycosidic angles of **1** may access a higher extent of conformational space than those of the natural compound, lentil, and daffodil lectins preferentially select the "natural" conformations around the glycosidic angles of the pseudotrisaccharide, behaving as a true glycomimetic, although probably with an entropy penalty to the recognition process.

Binding Studies. As a final step, the kinetics and binding properties of **1b** to Con A and daffodil lectins were studied and compared to those previously reported[50,52] for **1a.** SPR was used to monitor the binding and to allow the quantitative analysis of the molecular interactions, including association and dissociation rate constants, and thus ΔG of binding (see experimental). The binding abilities are characterized by the respective dissociation constants K_d, where $K_d = k_{off}/k_{on}$ (Table 5). The data show that both lectins do effectively interact with **1b**, with different relative affinities. Thus, **1b** is recognized by ConA with smaller affinity than **1a** (loss of binding free energy of almost 3 kcal/mol). This fact is not surprising, because as described above, all the three Man-residues are bound by the lectin, and due to the large conformational mobility of the glycomimetic, the entropy penalty to binding must be significant. In contrast, the binding affinity of **1b** by daffodil lectin is similar to that reported for the natural analogue **1a**, even somehow better. This similarity may also be explained by claiming the previously described "worst" recognition of branched versus linear trisaccharides by daffodil lectin. Only the external residues are bound by the protein, as shown by our NMR experiments, and the binding constant for daffodil/**1a** is significantly smaller than that for ConA/**1a**. Although merely speculative, and due to its inherent flexibility, the adaptability of **1b** to the daffodil binding site may be similar or slightly better than that of **1a**, thus providing a possible explanation for the observed moderate enhancement of the binding in this case. From the kinetic viewpoint, both lectins showed comparable off-rates for **1b**, whereas the on-rate was higher for ConA than that for daffodil, indicating a larger barrier for binding.

The data for the binding of ConA to **1b** is in agreement with other report described above in the Introduction for a mono C-glycosyl compound.[15] In other context, ΔG of binding of simple C-mannosyl and C-glucosyl derivatives to Con A has been previously compared to their O-analogues.[3bc] It was shown that both sets of compounds bind with similar affinities, although the specificity of binding decreased when the C-manno and C-gluco compounds were compared. The authors noticed that switching from an O- to a C-linkage can affect binding specificity in unpredictable ways, even if the change do not affects a region that directly interacts with the protein.[3bc]

Conclusions

The solution conformational properties of a complex *C*-trisaccharide has been carefully analyzed by a combination of NMR spectroscopy and time-averaged restrained molecular dynamics. It has been found that the glycosidic linkages around both the α-1 → 3- and the α-1 → 6-linkages show major conformational averaging. Indeed, several more conformations than those observed for the natural O-glycoside are observed, especially those occupying unusual Φ ca. 60° orientations for both Φ torsion angles. Surprisingly, a major conformational distinction between the natural compound **1a** and the glycomimetic **1b** affects to the behavior of ω_{16} torsion angle. This angle shows a major *gg* conformation for **1a**, with a substantial contribution of the *gt* rotamer. In contrast, **1b** shows basically a unique *gt* rotamer around this torsion. As recently established by Woods and co-workers,[41] the importance of solvation and polar effects for the establishment of a given conformation around ω angles of saccharide molecules is probably at the origin of the observed conformational change. Therefore, the substitution of the interglycosidic oxygen by a methylene group does not only affect the geometrical and stereoelectronic features of the molecule, but also the solvation features, that, in this case, affect to ω angle.

From a molecular recognition viewpoint, the occupancy of more conformations in **1b** yields an enhanced flexibility in solution compared to the parent O-glycoside. Despite this increased flexibility, the C-glycosyl analogue is still recognized by three mannose binding lectins, as shown by NMR and SPR methods. Moreover, a process of conformational selection takes place so that these lectins preferentially bind this glycomimetic **1b** similarly to the way they recognize the natural analogue. Depending on the architecture and extension of the binding site, and the adaptability of the ligand, loss or gain of binding affinity

with respect to the natural analogue may be found. Therefore, and as described for other C-glycosyl analogues, C-glycosyl compounds such as **1b** may be promising candidate to investigate other biologically relevant carbohydrate-protein interactions.

Experimental Section

Syntheses and Nomenclature. The C-trisaccharide **1b** and the C-disaccharides **2b** and **3b** were synthesized as described.[33] The glycosidic torsion angles are defined with respect to hydrogen atoms, as follows: Φ_{13}: H1′−C1′−C8−C3, Ψ_{13}: C1′−C8−C3−H3, Φ_{16}: H1″−C1″−C7−C6, Ψ_{16}: C1″−C7−C6−C5 and ω_{16}: C7−C6−C5−O5, where the nonreducing ends are labeled ′ and ″ for the 1 → 3- and the 1 → 6-linkage respectively (Scheme 1).

NMR Spectroscopy. The NMR experiments were performed at 500 MHz on Varian Unity and Bruker AVANCE spectrometers, between 299 and 318 K, and concentrations between 1 and 2 mM. Some experiments (T-ROESY of **1b**) were carried out on a Bruker AVANCE 700 MHz to get accurate NOE values. A 1D ^{1}H NMR spectrum of **1b** was carried out at 800 MHz to access the vicinal coupling constant values. The best *J* values were estimated by computer simulation of the 1D spectrum.

For the experiments with the free ligands, the corresponding compound was dissolved in D_2O and the solution was degassed by passing argon. COSY, TOCSY (80 ms, mixing time), and ge-HSQC experiments were performed using standard sequences at temperatures between 298 and 310 K, with 1−2 mM samples. 2D T-ROESY experiments (1 mM) were performed with mixing times of 300, 400, and 500 ms. Cross-peaks were integrated with the software provided by the manufacturer. All the 2D experiments were performed using a spectral width of 9.5 ppm for ^{1}H, with the rf carrier set at the residual HDO frequency. For ge-HSQC, the ^{13}C spectral width was of 100 ppm. The strenght of the 180° pulses during the spin lock period were attenuated four times with respect to that of the 90° hard pulses (between 7.2 and 7.5 μs). In most cases, including T-ROESY, cosine square window functions, were used for processing. To deduce the interproton distances, relaxation matrix calculations were performed using software written at home, available from the authors upon request.

For the bound ligands, legume lectins (*Concanavalin A.*, *Lens culinaris*, and *Narcissus pseudonarcissus*) were obtained from Sigma. STD and TRNOE experiments were performed at 500 MHz. First, the corresponding lectin was subjected to two cycles of freeze-drying with D_2O to remove traces of H_2O and transferred in solution to the NMR tube to give a final concentration of ca. 0.1−0.2 mM. TR−NOESY experiments were performed with mixing times of 150, 200, and 250 ms, for molar ratios between 17:1 and 34:1 of **1b**:lectin. The spectral width was 9.5 ppm and the rf carrier was set at the HDO frequency. No purging spin lock period to remove the protein signals background was employed. First, in all cases, line broadening of the sugar protons was monitored after the addition of the ligand. STD experiments were carried out by using the method proposed by Meyer, Peters, and coworkers.[47,48,51] No saturation of the residual HDO signal was employed and, again, no spin lock pulse was employed remove the protein signals background. In our hands, the use of a spin lock period induced artifacts in the difference spectrum. The theoretical analysis of the TRNOEs of the sugar protons was performed using a relaxation matrix with exchange, as described. Different exchange-rate constants, *k*, and leakage relaxation times were employed to obtain the optimal match between experimental and theoretical results of the intraresidue H-1/H-2 cross-peaks of the reducing Man moiety for the given protein/ligand ratio. Normalized intensity values were used since they allow correcting for spin-relaxation effects. The overall correlation time τ_c for the free state was always set to 0.23 ns and the τ_c for the bound state for lentil and daffodil were estimated as 30 and 15 ns, respectively. To fit the experimental TRNOE intensities, exchange-rate constants close to those determined by SPR were tested, with external relaxation times ρ^* for the bound state of 0.5−2 s were tested. TR−ROESY experiments were also carried out to exclude spin-diffusion effects. A continuous wave spin lock pulse was used during the 150 ms mixing time. Key NOEs were shown to be direct cross-peaks, since they showed different sign to diagonal peaks.

Molecular Mechanics and Dynamics Calculations. The initial molecular mechanics calculations were performed on both the C- and O-trisaccharide analogues (**1ab**), and their 1,3-disaccharide and the 1,6-disaccharide components (**2ab**, **3ab**) using the MM3* force field as implemented in Macromodel 4.5. Potential energy maps were calculated as described.[9,32,53] Some MD calculations were also performed with this force field. In particular, nine independent 1.5 ns unrestrained MD simulations were run starting from the combination of minima A−C with D−F. Additional molecular dynamics calculations of **1b** were done using the AMBER 5.0[31] force field. For the time-averaged-restrained molecular dynamics (tar-MD) the structures were constructed using the X-LEAP program.[54] All of the molecular dynamics simulations were carried out using the Sander module within the AMBER 5.0 package. The exact protocol for the tar-MD has been explicitly described elsewhere.[9,32]

In brief, they were carried out including a variable number of NOE-derived distances as time-averaged distance-constraints, and the key scalar coupling constants as a time-averaged couplings restraints. An $\langle r^{-6}\rangle^{-1/6}$ average was used for the distances, whereas a linear average was used for the coupling constants. To test the fit between experimental and produced values, the couplings were estimated from the calculated torsion angles (θ) by using the well-known Karplus equation: $J = A\cos^2\theta + B\cos\theta + C$. The values of *A*, *B*, and *C* were chosen to fit the extended Karplus−Altona relationship.

Surface Plasmon Resonance

F1 chip, HBS buffer, and EDC/NHS were from Biacore. All other chemical was obtained from Sigma. Buffers were filtered and deoxygenated. The version 3.2 software was used.

Immobilization of Lectin on F1 Chips. Because amine coupling is the most common immobilize method in SPR, a thin layer of carboxymethylated dextran, covering the surface of the gold film in the sensor chip, was used to facilitate the immobilization of the ligand via reaction of primary amino groups on the protein with EDC and NHS. This carboxymethylated dextran layer also provides a hydrophilic environment for the interaction of biological molecules. After ligand coupling, ethanolamine was added to deactivate remaining active esters. Thus, *Concanavalin A.* and *Narcissus pseudonarcissus* lectins were covalently bound to the sensor surface through its primary amino groups following this strategy. The carboxymethylated dextran surface (F1 sensor chips) was first activated using a 7 min (35 μL) injection pulse of an equimolar mix of *N*-hydroxysuccinimide (NHS) and *N*-ethyl-*N*-(dimethyaminopropyl) carbodiimide (final concentration is 0.05 M, mixed immediately prior to injection). The surface was cleaned with the extraclean step available in the instrument in order to be sure that all the lines were cleaned. The lectin solution, (80 μL of 80 μg/mL in sodium citrate buffer 3 mM, pH = 6.0) was

(53) For instance, (a) Espinosa, J.-F.; Bruix, M.; Jarreton, O.; Skrydstrup, T.; Beau, J.-M.; Jiménez-Barbero, J. *Chem. Eur J.* **1999**, *5*, 442. (b) Poveda, A.; Asensio, J. L.; Polat, T.; Bazin, H.; Linhardt, R. J.; Jiménez-Barbero, J. *Eur. J. Org. Chem.* **2000**, 1805−1813, and references therein. (c) For a description of the application of calculations to carbohydrate conformation, see French, A. D.; Brady, J. W. *Computer Modelling of Carbohydrate Molecules*; American Chemical Society Symposium Series; Washington D.C., 1990.

(54) Schafmeister, C. E. A. F.; Ross, W. S.; Romanovski, V. *LEAP*; University of California: San Francisco, 1995.

then injected by manual injection. Excess unreacted sites on the sensor surface were blocked with a 35 μL injection of 1 M ethanolamine. The surface was cleaned with the extraclean step available in the instrument to be sure that all the lines were cleaned.

Kinetic Measurement of the Lectin Interaction with the Oligosaccharides via SPR. A 15 μL injection of samples (at 1−0.2 mM) in HBS buffer was made at a flow rate of 5 μL/min. At the end of the sample plug, the same buffer was flowed over the sensor surface to facilitate dissociation. After a suitable dissociation time, the sensor surface was regenerated for the next sample using a 10 μL pulse of 10 mM H_3PO_4. The response was monitorized as a function of time (sensogram) at 25 °C. Kinetic parameters were evaluated using the BIA Evaluation software (version 3.0.2, 1999). A plot of k_s versus the protein concentration from the association phase yielded the association rate constants (k_{on}). The dissociation rate constants (k_{off}) were obtained from the direct analysis of the dissociation phase of the sensograms. The binding abilities are characterized by the respective dissociation constants K_d, where $K_d = k_{off}/k_{on}$ (Table 5).

The successful immobilization of *Concanavalin A.* and *Narcissus pseudonarcissus* on F1 was confirmed by the observation of a 3276 RU and 780 RU increased in the sensor chip, respectively. The proteins were stable on the sensor surface because more than 90% of the reactivity remained even after 10 repeated injections of proteins, and regeneration using 10 mM H_3PO_4.

A test was also made to compare the binding of the natural analogue **1a** to daffodil lectin to that described in the literature. The SPR-based Kd found was of the same order of magnitude (mM) than that previously described.[52]

Acknowledgment. Financial support by the Ministry of Science and Technology of Spain is gratefully acknowledged (DGES, BQU-2000-C1501-C01). We thank Dr. J. L. Asensio (CSIC, Madrid) for helpful discussions regarding the tar-MD simulations, and Dr. A. Poveda (UAM, Madrid), M. Gairí (UB, Barcelona), and P. Nieto (CSIC, Seville) for recording some of the NMR spectra. The NMR facility at the University of Barcelona is thanked by the access to the 800 MHz spectromer. This paper is dedicated to Prof. Julio Delgado Martín (CSIC, Seville) on occasion of his 60th birthday.

Supporting Information Available: Preliminary analysis of the NMR features (Figure S1) of the C-trisaccharide and its constituent C-disaccharides; assignment of the stereochemistry of the methylene protons; molecular mechanics analysis of 1b, 2b, and 3b; Tables S1−S3 and Figures S1−12. This material is available free of charge via the Internet at http://pubs.acs.org.

JA020468X